



**QUEEN'S
UNIVERSITY
BELFAST**

A Burkholderia Type VI Effector Deamidates Rho GTPases to Activate the Pyrin Inflammasome

Aubert, D. F., Xu, H., Yang, J., Shi, X., Gao, W., Li, L., Bisaro, F., Chen, S., Valvano, M. A., & Shao, F. (2016). A Burkholderia Type VI Effector Deamidates Rho GTPases to Activate the Pyrin Inflammasome. *Cell host & microbe*, 19(5), 664-674. <https://doi.org/10.1016/j.chom.2016.04.004>

Published in:
Cell host & microbe

Document Version:
Peer reviewed version

Queen's University Belfast - Research Portal:
[Link to publication record in Queen's University Belfast Research Portal](#)

Publisher rights

© 2016 Elsevier [B. V.] [Ltd.] This manuscript version is made available under the CC-BY-NC-ND 4.0 license <http://creativecommons.org/licenses/by-nc-nd/4.0/>, which permits distribution and reproduction for non-commercial purposes, provided the author and source are cited.

General rights

Copyright for the publications made accessible via the Queen's University Belfast Research Portal is retained by the author(s) and / or other copyright owners and it is a condition of accessing these publications that users recognise and abide by the legal requirements associated with these rights.

Take down policy

The Research Portal is Queen's institutional repository that provides access to Queen's research output. Every effort has been made to ensure that content in the Research Portal does not infringe any person's rights, or applicable UK laws. If you discover content in the Research Portal that you believe breaches copyright or violates any law, please contact openaccess@qub.ac.uk.

**A *Burkholderia* Type VI Effector Deamidates Rho GTPases to Activate
the Pyrin Inflammasome**

**Daniel F. Aubert^{1¶}, Hao Xu^{2¶}, Jieling Yang^{2, 4¶}, Xuyan Shi², Wenqing Gao², Lin Li²,
Fabiana Bisaro³, She Chen² Miguel A. Valvano^{1, 3*}, and Feng Shao^{2, 5*}**

¹ Department of Microbiology and Immunology, University of Western Ontario, London,
N6A 5C1, Canada.

² National Institute of Biological Sciences, Beijing 102206, China.

³ Centre for Infection and Immunity, Queen's University Belfast, Belfast, BT9 7AE,
United Kingdom.

⁴ National Laboratory of Biomacromolecules, Institute of Biophysics, Chinese Academy
of Sciences, Beijing 100101, China.

⁵ National Institute of Biological Sciences, Beijing, Collaborative Innovation Center for
Cancer Medicine, Beijing 102206, China.

[¶] Equal contribution

* Correspondence: m.valvano@qub.ac.uk (M.A.V), shaofeng@nibs.ac.cn (F.S.).

21 Article Highlights

22

23

24 ● *B. cenocepacia* employs a type VI effector TecA to disrupt actin cytoskeleton

25 ● TecA inactivates Rho GTPases by deamidating Asn-41 in RhoA

26 ● TecA defines a family of bacterial proteins with asparagine deamidase activity

27 ● TecA deamidation of Rho GTPases triggers Pyrin inflammasome activation

28 ● Detection of TecA by Pyrin protects mice from lethal *B. cenocepacia* infection

29

SUMMARY

Burkholderia cenocepacia employs a Type VI secretion system (T6SS) to survive in macrophages by disarming Rho-type GTPases, causing actin cytoskeletal defects. Here, we identified TecA (T6SS effector affecting cytoskeletal architecture), a non-VgrG T6SS effector responsible for disrupting actin cytoskeleton. TecA and other bacterial homologs bear a cysteine protease-like catalytic triad, which inactivates Rho GTPases by catalyzing deamidation of a specific asparagine in Rho. TecA deamidation of Rho activates the canonical inflammasome and pyroptotic cell death in infected macrophages and dendritic cells, which is mediated by the familial Mediterranean fever disease protein Pyrin. The physiological function of TecA is recapitulated in mouse lung infections, in which its deamidase activity is necessary and sufficient for *B. cenocepacia*-triggered lung inflammation. Detection of TecA by Pyrin is protective on mice from lethal *B. cenocepacia* infection. Therefore, *Burkholderia* TecA is a novel T6SS effector that modifies a eukaryotic target through a unique asparagine deamidase activity, which elicits host cell death and inflammation due to activation of the Pyrin inflammasome.

INTRODUCTION

The type VI-secretion system (T6SS) is a contractile nanomachine widely distributed in Gram-negative bacteria (Basler et al., 2012; Boyer et al., 2009; Clemens et al., 2015; Kudryashev et al., 2015; Zoued et al., 2014). The T6SS structurally resembles the bacteriophage tail injection device; the tail tube is made of the Hcp protein and a puncturing device containing proteins of the VgrG family and various VgrG-associated proteins caps the Hcp tube (Zoued et al., 2014). Upon cell contact, the T6SS delivers toxic effectors into neighboring target cells. Most of the known T6SS effectors act on bacterial competitors cells and include peptidoglycan-, membrane-, and nucleic acid-targeting enzymes (Durand et al., 2014; Russell et al., 2014).

Among T6SS effectors that act on eukaryotic cells, the "evolved" VgrG proteins (also required for assembly of the T6SS apparatus) are the most established. The *P. aeruginosa* VgrG2b contains a Zn^{2+} -dependent metalloprotease domain and interacts with tubulin components (Sana et al., 2015), while VgrG1 proteins from *Vibrio cholerae* and *Aeromonas hydrophila* contain an actin cross-linking domain (Durand et al., 2012) and an ADP-ribosylating domain (Suarez et al., 2010), respectively. Other evolved VgrGs from *V. parahaemolyticus* and *B. pseudomallei* have effects on autophagy and host cell fusion (Schwarz et al., 2014; Toesca et al., 2014; Yu et al., 2015) with unknown molecular mechanisms. In contrast, few non-VgrG T6SS effectors have been reported. The VasX protein from *V. cholerae* contains an N-terminal pleckstrin domain that interacts with phospholipids and can compromise the inner membrane of prokaryotic target cells (Miyata et al., 2011; Miyata et al., 2013); the PldA/B proteins from *P. aeruginosa* are phospholipases and their expression is associated with PI3K/Akt activation in infected

eukaryotic cells (Jiang et al., 2014); EvpP from *Edwardsiella tarda* is necessary for virulence of the bacteria (Zheng and Leung, 2007). However, the physiological function of these non-VgrG effectors is not well established and it remains to be conclusively demonstrated that these proteins are bona fide T6SS effectors specifically modulating eukaryotic host functions.

Burkholderia cenocepacia is an environmental Gram-negative opportunistic pathogen that causes severe chronic lung infection in cystic fibrosis patients (Drevinek and Mahenthiralingam, 2010). *B. cenocepacia* is pathogenic in plant and non-mammalian animal infection models (Khodai-Kalaki et al., 2015; Uehlinger et al., 2009; Vergunst et al., 2010), and survives intracellularly within amoebae and macrophages (Valvano et al., 2012). Unlike other cystic fibrosis pathogens, *B. cenocepacia* does not form biofilms in the lungs of infected patients and resides primarily within human mucosal macrophages (Schwab et al., 2014). Intramacrophage *B. cenocepacia* delays phagosomal maturation, alters the actin cytoskeleton, and triggers inflammation and cell death (Valvano et al., 2012). *B. cenocepacia* infection and pathogenesis critically requires the function of a T6SS. The *B. cenocepacia* T6SS inactivates Rho family GTPases, which reduces the phagocytic capacity of macrophages (Flannagan et al., 2012; Rosales-Reyes et al., 2012), blocks NADPH oxidase assembly onto the *B. cenocepacia*-containing vacuole (Keith et al., 2009; Rosales-Reyes et al., 2012), and disrupts the macrophage's actin cytoskeleton (Aubert et al., 2008; Flannagan et al., 2012; Rosales-Reyes et al., 2012). The T6SS also leads to activation of the canonical caspase-1 inflammasome, interleukin (IL)-1/18 secretion and pyroptosis in macrophages (Gavrilin et al., 2012; Xu et al., 2014). Pyroptosis is a programmed, necrotic cell death that causes exaggerated proinflammatory

responses and ultimately tissue damage. Inflammasome activation after *B. cenocepacia* infection in macrophages involves Pyrin (Xu et al., 2014), an intracellular innate immune sensor that detects pathogen-induced modifications of Rho GTPases (Xu et al., 2014; Yang et al., 2014). Interestingly, gain-of-function mutations in Pyrin are the cause for familial Mediterranean fever, an autoinflammatory disease in humans.

Despite the genetic requirement of the T6SS in *B. cenocepacia* for manipulating host function, no T6SS effectors involved in the cellular changes of infected macrophages have been identified. In fact, no effector-encoding genes appear to be present in the T6SS core cluster and neither the candidate VgrG nor VgrG-associated proteins are responsible for the actin cytoskeletal rearrangements (Aubert et al., 2015). Here, we performed genetic screen in *B. cenocepacia* and identified TecA (T6SS effector protein affecting cytoskeletal architecture), a non-VgrG T6SS effector with a unique deamidase activity. Specific deamidation by TecA of a critical asparagine residue in RhoA and Rac1 GTPases causes their inactivation and disruption of host actin cytoskeleton. TecA defines a novel family of bacterial cysteine protease-like enzymes that catalyze asparagine deamidation of Rho GTPases. TecA deamidation of RhoA drives activation of the Pyrin inflammasome in infected macrophages and dendritic cells. This innate immune response mediates lung inflammation during intranasal *B. cenocepacia* infection in mice, and can also protect the mice from lethal peritoneal *B. cenocepacia* infection. TecA is the first bacterial toxin secreted by an intracellular pathogen that targets the switch I region of Rho GTPases and inactivates their function by deamidation of an essential asparagine residue.

RESULTS

Identification of a non-VgrG T6SS effector in *B. cenocepacia* that drives host actin cytoskeleton rearrangements

B. cenocepacia infection disrupts the actin cytoskeleton in macrophages, forming “beads on a string”-like structures featuring long extensions with bleb-like structures located along the extensions and surrounding the cell periphery (Aubert et al., 2008; Flannagan et al., 2012; Rosales-Reyes et al., 2012). This phenotype reflects a collapse of the actin filaments in the lamellipodia and defective retraction during migration, and is dependent upon a functional T6SS (Aubert et al., 2008; Flannagan et al., 2012; Rosales-Reyes et al., 2012). The T6SS activity in *B. cenocepacia* can be stimulated by deleting *AtsR* (Adhesion and Type Six secretion system Regulator), a hybrid sensor kinase of a two-component system (Aubert et al., 2010; Aubert et al., 2008; Aubert et al., 2013; Khodai-Kalaki et al., 2013). This ensures uniform high expression of the T6SS genes and provides higher reproducibility of the results, especially in strain K56-2 that does not have a high macrophage infection index. Consistently, infection of macrophages with the $\Delta atsR$ mutant of *B. cenocepacia* K56-2 results in increased formation of “beads on a string”-like structures (Aubert et al., 2008; Flannagan et al., 2012; Rosales-Reyes et al., 2012). We recently developed a densitometry assay that quantifies the extent of this phenotype (Aubert et al., 2015). Using this assay, we performed random transposon mutagenesis screens in the $\Delta atsR$ background to search for bacterial mutants unable to induce disruption of the actin cytoskeleton in macrophages. 27 mutants were identified from the initial screen of 2,700 independent transposon mutants, and 6 of them (all having transposon insertions outside of the T6SS cluster) did not pass further

confirmation by targeted deletion of the gene disrupted by the transposon. Among the remaining 21 mutants incapable of inducing “beads on a string”-like structures, 20 had a transposon inserted into genes encoding critical core components of the T6SS apparatus (Figure 1A). The last insertion mutant was in BCAM1857 (GenBank: CAR55715.1), a gene located on chromosome 2 and outside of the T3SS locus (Figure 1A). Deletion of BCAM1857 in $\Delta atsR$ resulted in a strain unable to induce formation of the “beads on a string”-like structures in macrophages (Figure 1B-C). This phenotype could be restored to parental levels by introducing in the strain a plasmid expressing the BCAM1857 protein (Figure 1B-C). Therefore, BCAM1857 could be a putative non-VgrG T6SS effector responsible for cytoskeletal changes in macrophages and was renamed TecA (T6SS effector protein affecting cytoskeletal architecture).

Growth curves and gentamicin protection assays indicated that *B. cenocepacia* $\Delta atsR\Delta tecA$ grows at a similar rate as the $\Delta atsR$ parent strain in LB medium as well as in immortalized murine macrophages (Figure S1A and S1B). Similar Hcp levels were detected in $\Delta atsR$ and $\Delta atsR\Delta tecA$ culture supernatants, indicating that deletion of *tecA* does not affect the T6SS apparatus (Figure S1C). When overexpressed in $\Delta atsR$ and the isogenic T6SS-deficient $\Delta atsR\Delta hcp$ mutant, low amounts of TecA were predominantly and reproducibly detected in culture supernatants of $\Delta atsR$ but not $\Delta atsR\Delta hcp$ despite a similar TecA expression found in cell lysates of the two bacterial strains (Figure S1C). Chromosomally encoded TecA was not detectable initially in $\Delta atsR$ cell lysates by the routine immunoblotting assay (Figure S1C), but became detectable upon increasing sample loading and exposure time of the immunoblot (Figure S1D), suggesting a low

expression of TecA in *in vitro* cultured bacteria. Together, these data suggest the need of a functional T6SS for TecA secretion, as expected for a bona fide T6SS effector protein.

Like *B. cenocepacia* K56-2, *B. multivorans* ATCC17616 also infects, survives and replicates within macrophages (Schmerk and Valvano, 2013). *B. multivorans* ATCC17616 possesses two T6SS clusters and an *atsR* ortholog (Bmul_5222, herein named *atsR_{Bm}*), but lacks a *tecA* homolog. Culture supernatant of *B. multivorans* ATCC17616 Δ *atsR_{Bm}* showed a similar expression of Hcp as that of *B. cenocepacia* K56-2 Δ *atsR*, suggesting that the T6SSs in *B. multivorans* ATCC17616 are functional (Figure S1E). However, Δ *atsR_{Bm}* could not induce the “beads on a string”-like phenotype in infected macrophages (Figure 1D). Notably, heterologous expression of TecA in Δ *atsR_{Bm}* enabled this bacterium to induce cytoskeletal rearrangements comparable to those found in *B. cenocepacia* (Figure 1C-D). These data strongly indicate that T6SS-translocated TecA is both necessary and sufficient to drive cytoskeletal defects in infected macrophages.

***B. cenocepacia* infection induces Asn-41 deamidation of RhoA due to a putative T6SS effector activity**

B. cenocepacia K56-2 and J2315 are clonally related and often used indistinctly (Mahenthiralingam et al., 2000). Unlike K56-2, J2315 lacks the ability to produce O antigen lipopolysaccharide (Ortega et al., 2005) and consequently infects macrophages more readily (Saldías et al., 2009). J2315 can induce similar “beads on a string”-like structures in macrophages, which does not require deletion of *atsR*. We recently discovered that intracellular J2315 infection resulted in the T6SS-dependent inactivation

of RhoA by inducing deamidation of asparagine-41 (Asn-41) (Xu et al., 2014), a residue located in the switch-I region of the GTPase. This observation was confirmed here by mass spectrometry analyses of FLAG-RhoA purified from murine dendritic DC2.4 cells infected with J2315 or its T6SS-defective Δhcp mutant (Figure 2A). The *C. botulinum* ADP-ribosylation C3 toxin modifies Asn-41, generating a mobility shift of RhoA on SDS-polyacrylamide gels. This mobility shift provided a convenient assay, which confirmed the deamidation modification of RhoA induced J2315 infection (Figure 2A). Notably, we observed that RhoA from non-infected cells, upon incubation with cytosolic extracts of J2315 but not its ΔHcp mutant-infected cells, also resisted C3 toxin modification (Figure 2B). The Rho-modifying activity could also be recapitulated from the pellets of J2315-infected macrophages (containing the bacteria and proteins expressed within the bacteria), but unlike the situation in the bacteria-free cytosol, the activity was not dependent on the T6SS (Figure 2C). Together, these data strongly indicate that *B. cenocepacia* expresses a T6SS effector that deamidates RhoA upon translocation from the bacteria into the host cytosol, also excluding the possibility that infection-induced RhoA deamidation is host-derived. Supporting this idea, we found that lysates of *in vitro* cultured *B. cenocepacia*, but not those of *E. coli* and *B. thailandensis*, showed a similar activity that renders RhoA resistant to further modification by the C3 toxin (Figure 2D). Consistently, RhoA recombinantly expressed and purified from *B. cenocepacia* showed a deamidation modification on Asn-41, contrasting to recombinant RhoA purified from the conventional *E. coli* host (Figure 2E).

The T6SS effector TecA mediates RhoA deamidation *in vivo* and *in vitro*

Also in the experiments described above, we found that RhoA purified from the $\Delta tecA$ strain of *B. cenocepacia* was not deamidated and showed the same mass as that from *E. coli* (Figure 2E), suggesting that TecA is the candidate T6SS effector that causes RhoA deamidation. We further observed that deamidation of RhoA did not occur in DC2.4 cells infected with the $\Delta tecA$ isogenic mutant of J2315, similarly as in infections with the Δhcp mutant (Figure 3A). Complementing TecA expression in $\Delta tecA$ by a *tecA*-encoding plasmid restored the protection of RhoA from C3 toxin-catalyzed ADP-ribosylation (Figure 3B). Further, introducing the TecA-expression plasmid in *B. thailandensis*, which harbors a similar T6SS, resulted in the same modification of RhoA upon infection of DC2.4 cells, which did not occur in cells infected with bacteria expressing the enzymatically inactive TecA_{C41A} (see below) (Figure 3C). These results demonstrate that TecA is essential for the T6SS-mediated Asn-41 deamidation of RhoA. Exogenous expression of TecA, but not TecA_{C41A}, in 293T cells recapitulated the same results as those observed in infected DC2.4 cells (Figure 3D). Mass spectrometry of FLAG-RhoA purified from 293T cells confirmed the conversion of Asn-41 into an aspartic acid (Figure 3E). Same results were observed in *E. coli* co-expressing RhoA and the TecA or TecA_{C41A} proteins (Figure 3F). These data demonstrate that TecA is required and sufficient for deamidation of the Asn-41 residue in RhoA.

Previous work showed that the *B. cenocepacia* T6SS is needed to deactivate the Rho-family Rac1 and Cdc42 GTPases (Flannagan et al., 2012; Rosales-Reyes et al., 2012). We therefore investigated Rac1 expressed in 293T cells together with TecA. Mass spectrometry confirmed that the peptide containing Asn-39 in Rac1 (equivalent to Asn-41 in RhoA) was modified to aspartic acid by TecA (Figure 3G), indicating TecA causes the

same modification in other Rho-family members by targeting the conserved asparagine in the switch I region. Notably, when we transiently expressed the deamidated Rac1 (N39D) or RhoA (N41D) alone in 293T cells, the “beads on a string”-like structure was readily observed in cells expressing Rac1 N39D but not RhoA N41D (Figure 3H). These suggest that TecA-induced Rac1 deamidation and inactivation is responsible for the actin cytoskeleton disruption caused by *B. cenocepacia* infection.

The TecA effector defines a family of bacterial deamidases that modify Rho GTPases

TecA is a 159-amino acid protein of predicted unknown function. As expected for a T6SS substrate, TecA lacks a canonical N-terminal signal peptide. No putative conserved domains could be detected using PFAM and HHPred, and we also failed to identify any evident primary sequence similarity between TecA and known deamidases or other enzymes with hydrolytic activity. BLAST searches uncovered TecA orthologs in *B. cenocepacia* BC7, H111, AU1054, HI2424, H111, and MC0-3, (sharing over 91-99% amino acid identity with TecA of K56-2 and J2315), and in *B. contaminans*, *B. pyrrocinia*, *B. lata*, *B. cepacia* ATCC25416, *B. cenocepacia* PC184, and *B. ubonensis* (sharing 75-85% amino acid identity with TecA) (Figure 4A), suggesting that TecA is prevalent in a subset of *Burkholderia* species. Several additional homologs, sharing from 37 to 50% amino acid identity with TecA were also found in *Alcaligenes faecalis*, *Chryseobacterium indologenes*, the fish pathogen *Flavobacterium branchiophilum* FL-15, and the opportunistic pathogen and symbiont *Ochrobactrum anthropi* ATCC49188 (Figure 4A). Sequence alignments of these proteins revealed a conserved Cys-His-Asp

triad (Cys-41, His-105, and Asp-148 in TecA). The Cys-His-Asp/Asn/Glu/Gln triad forms a catalytic pocket in many proteases and protease-like hydrolytic enzymes including deamidases (Cui et al., 2010; Washington et al., 2013; Yao et al., 2012). The cysteine, activated by the histidine and sometimes the nonessential third residue in the triad, serves as the catalytic nucleophile. Interestingly, *in silico* structural modeling of TecA using I-TASSER (Roy et al., 2010) revealed a similar structural fold with various cysteine protease families including proteins containing the NlpC/P60, cysteine-histidine hydrolase, and papain-like cysteine peptidase domains (PDB accessions 2EVR, 2FG0, 2HBW, 4F88, 3GQJ, and 3S0Q). The predicted TecA model revealed the putative catalytic Cys-41 and His-105 residues situated in positions consistent with a catalytic triad typical of cysteine proteases and protease-like hydrolases, further supporting the hypothesis that TecA is a cysteine protease-like hydrolase (Figure 4B). Thus, despite the lack of significant primary sequence similarity, TecA likely adopts a three-dimensional fold characteristic of members of the cysteine protease family.

Mutagenesis was then carried out to test the deamidase activity of TecA and its orthologs. Alanine substitution of Cys-41 and His-105 in TecA abrogated Asn-41 deamidation of RhoA and Rac1 in the 293T cells co-expression system (Figure 5A and Figure 3D, 3E and G). The TecA_{D148A} was partially active, but removal of the C-terminal 20 residues containing the Asp-148 resulted in a completely inactive enzyme (Figure 5A). TecA_{C41A} was also unable to deamidate Asn-41 in RhoA in the *E. coli* expression assay (Figure 3F). Upon DC2.4 infection with *B. cenocepacia* or *B. thailandensis* strains expressing the T6SS, TecA_{C41A} failed to induce RhoA deamidation (Figure 3C and data not shown). Co-expression of RhoA and TecA orthologues from *C. indologenes*

(WP_034735953), *F. branchiophilum* (WP_014085254), and *O. anthropi* (WP_011982319) in 293T cells gave the same results as with *B. cenocepacia* TecA, namely protection of RhoA from C3 toxin-mediated ADP-ribosylation (Figure 5B). Further, replacement of the putative catalytic Cys-40, His-104, or Asp-149 in WP_034735953 with alanine abrogated the protective effect on RhoA from C3 toxin-catalyzed modification (Figure 5C). Mass spectrometry confirmed that WP_034735953 deamidated RhoA and Rac1 in 293T cells at Asn-41 and Asn-39, respectively, and this modification did not occur with the C40A mutant protein (Figure 5D). Together, these results demonstrate that *B. cenocepacia* TecA epitomizes a family of bacterial proteins specifically catalyzing asparagine deamidation of Rho GTPases in mammalian cells.

TecA deamidation of RhoA mediates *B. cenocepacia*-induced Pyrin inflammasome activation

Our recent studies suggest that the Pyrin inflammasome senses Rho inactivation induced by bacterial Rho-modifying agents (Xu et al., 2014). Therefore, we examined whether TecA deamidation of host Rho GTPases could activate the Pyrin inflammasome. Confirming our previous observation (Xu et al., 2014), infection of primary mouse bone marrow macrophages (BMDMs) with *B. cenocepacia* J2315, but not the Δhcp mutant, stimulated caspase-1 autoprocessing, pyroptotic cell death and IL-1 β secretion (Figure 6A and 6B), hallmarks of canonical inflammasome activation. These proinflammatory responses were absent in BMDMs derived from *Mefv*^{-/-} mice (*Mefv* is the gene encoding Pyrin). Importantly, the $\Delta tecA$ mutant strain behaved similarly as Δhcp , failing to induce caspase-1 activation, pyroptosis and IL-1 β secretion (Figure 6A and 6B). Restoring TecA

expression in $\Delta tecA$ restored *B. cenocepacia*-induced caspase-1 activation and pyroptosis in primary BMDMs (Figure 6C and 6D). In contrast, TecA mutants in the three putative catalytic residues (C41A, H105A and D148A) did not restore the infection-triggered inflammasome responses (Figure 6C and 6D). Similar results were obtained with *B. cenocepacia* infections in DC2.4 cells (Figure 6E). Furthermore, we generated the N41L mutant of RhoA as well as the equivalent N39L mutants of Rac1 and Cdc42. When the deamidation-resistant mutant Rho was overexpressed in DC2.4 cells, we found that RhoA N41L could evidently inhibit *B. cenocepacia* infection-induced Pyrin inflammasome activation (Figure 6F). In contrast, neither the N39L mutants of Rac1/Cdc42 nor wild-type RhoA showed such dominant-negative effects (Figure 6F). These data are consistent with our previous observation that modification of RhoA but not other GTPase substrates induces Pyrin inflammasome activation (Xu et al., 2014), and strongly suggest that TecA-mediated deamidation of RhoA is responsible for *B. cenocepacia*-stimulated Pyrin inflammasome activation.

TecA mediates *B. cenocepacia*-induced lung inflammation and its recognition by Pyrin can protect mice from lethal infection

Intranasal *B. cenocepacia* infection of wild-type mice triggered strong lung inflammation, evidenced by massive infiltration of inflammatory cells, appearance of intra-alveolar leukocytes, and destruction of the normal lung architecture due to activation of the Pyrin inflammasome (Xu et al., 2014) (Figure 7A). In contrast, mice infected with *B. cenocepacia* $\Delta tecA$ showed negligible lung inflammation. Expressing wild type but not the deamidase-defective TecA_{C41A} protein in the mutant bacteria restored the strong

inflammation in the infected lungs (Figure 7A). These observations were also evident from the clinical pathology scores that measure the lung damage (Figure 7B). Thus, the TecA deamidase activity induces Pyrin inflammasome-mediated inflammation due to its modification and inactivation of host Rho GTPases. To further demonstrate the functional significance of this innate immune recognition, peritoneal infection of mice with *B. cenocepacia* was performed. At the infection dose of 2×10^8 bacteria, nearly all the mice could resist wild-type *B. cenocepacia* infection, but the large majority of infected mice succumbed to the $\Delta tecA$ mutant bacteria (Figure 7C). The lethality is presumably caused by loss of the inflammation and consequently attenuated control of bacterial replication in the mice. Consistently, a higher number of *B. cenocepacia* $\Delta tecA$ than that of wild-type bacteria was recovered from the spleen of infected mice (Figure 7D). The bacterial loads in the liver showed a similar trend despite that the difference was not statistically significant. When the infection was performed with the *Mefv*^{-/-} mice, wild-type *B. cenocepacia* infection also became lethal and showed a comparable lethality as the $\Delta tecA$ mutant bacteria (Figure 7C). These results highlight the protective role of Pyrin inflammasome that functions through detecting the Rho deamidase activity of TecA in *B. cenocepacia*.

DISCUSSION

We show that TecA is a single, non-VgrG T6SS effector protein that elicits actin cytoskeletal defects, inflammation, and macrophage pyroptosis by inactivating Rho GTPases through deamidation of an asparagine residue within the GTPase switch I region. Rho GTPases are central molecular switches of eukaryotic cells that cycle

between the inactive GDP-bound and active GTP-bound states and regulate key signaling pathways concerning cytoskeletal dynamics, trafficking, immune responses, and cell proliferation (Aktories, 2011). Not unexpectedly, many microbes produce proteins that target Rho GTPase signaling either by direct covalent modification of the GTPases or by manipulating their upstream and downstream regulators and effectors (Aktories, 2011). Pathogen effectors can block Rho GTPases activation, causing inhibition of cell migration and phagocytosis and disruption of the actin cytoskeleton, while in other cases can activate the GTPases to mediate bacterial entry into the cytosol. Alteration of the actin cytoskeletal dynamics is a typical cellular response to both inactivated and activated Rho GTPases, and recent evidence suggests that pathogen-induced "unnatural" actin dynamics is sensed by host innate immunity. For example, activation of Rac1/Cdc42 by the *Salmonella enterica* Type III effector SopE stimulates host NOD1 signaling leading to the induction of NF- κ B-dependent inflammatory responses (Keestra et al., 2013), while RhoA inactivation causes Pyrin inflammasome activation (Xu et al., 2014).

TecA defines a new family of bacterial deamidases that are deployed by the T6SS upon bacterial intracellular infection. Enzymatic deamidation is a common pathogenic strategy utilized by a broad range of bacterial pathogens that infect plants and animals (Washington et al., 2013). Deamidation causes the replacement of an amide group with a carboxylate group, converting glutamine and asparagine into glutamic acid and aspartic acid, respectively. Several families of bacterial deamidases are known, which target various eukaryotic proteins that play key roles in cellular physiology. *E. coli* (CNF1, CNF2, CNF3) and *Yersinia pseudotuberculosis* (CNFY) cytotoxic necrotizing factors (Flatau et al., 1997; Lockman et al., 2002; Schmidt et al., 1997) and the *Vibrio*

parahaemolyticus type III effector VopC (Zhang et al., 2012) target a glutamine residue in the switch II domain of Rho GTPases, which leads to constitutive activation resulting in cytoskeletal rearrangements. BLF1 is a lethal toxin from *B. pseudomallei* that inhibits host protein synthesis via deamidation of the translation factor eIF4A (Cruz-Migoni et al., 2011). *Pasteurella multocida* toxin PMT activates heterotrimeric G proteins affecting several downstream signaling pathways (Orth et al., 2009). Further, cell cycle-inhibiting factors from multiple bacterial species inhibit ubiquitination pathways by deamidating Glu-40 of ubiquitin and the ubiquitin-like protein NEDD8 (Cui et al., 2010), while *Shigella flexneri* has evolved a type III effector protein that dampens TRAF6-mediated immune responses by deamidating UBC13 (Sanada et al., 2012). It is worth noting that TecA is the first known bacterial deamidase with specificity for asparagine and an inhibitory effect on Rho GTPases.

TecA and its orthologs do not share primary amino acid sequence homology with other known bacterial deamidases, and represent a novel class of deamidases. The TecA family has a putative catalytic triad consisting of invariant cysteine, histidine and aspartic acid residues, characteristic of the papain-like superfamily of hydrolytic enzymes (Washington et al., 2013). Like other bacterial deamidases acting on Rho GTPases such as CNF1 and CNFY, both RhoA and Rac1 can be TecA substrates. Previous data indicate that Cdc42 is inactivated by the *B. cenocepacia* T6SS in murine macrophages (Flannagan et al., 2012; Rosales-Reyes et al., 2012), suggesting that this GTPase might also be a TecA substrate. As with CNFI (Flatau et al., 2000), TecA likely recognizes a relatively short, common structural element in the switch-I region that would explain its ability to

work with multiple substrates, but additional experimentation is required to investigate this hypothesis.

Deamidation is enzymatically irreversible, making deamidases potent virulence factors (Washington et al., 2013). This is underscored by the robust effect of TecA on the innate immune responses and inflammation, as we have observed in infected macrophages and mice. The pro-inflammatory potential of *B. cenocepacia* has long been recognized, especially in the context of cystic fibrosis (Abdulrahman et al., 2011; Downey et al., 2007; Kopp et al., 2012). Our results convincingly demonstrate that lung inflammation upon *B. cenocepacia* infection depends on an enzymatically active TecA and highlight the importance of the Pyrin inflammasome in innate immune detection of *B. cenocepacia* (Xu et al., 2014). Indeed, Pyrin responds to pathogen modification and inactivation of Rho GTPases, which echoes the “guard hypothesis” in plant immunity (Xu et al., 2014; Yang et al., 2014). The effect of TecA-mediated Rho deamidation on the actin cytoskeleton of *B. cenocepacia*-infected cells and the fact that Pyrin and the Pyrin-ASC complexes localize to actin filaments (Mansfield et al., 2001; Waite et al., 2009), strongly suggest that Pyrin could be a sensor for actin homeostasis. In this context, the identification of TecA also provides a tool for future dissection of the pathway leading to Pyrin inflammasome activation.

EXPERIMENTAL PROCEDURES

Bacterial strains and plasmids

Strains and plasmids used in this study are listed in Table S1. Details on bacterial growth conditions, DNA transformation and triparental mating, and the cloning of TecA, RhoA and Rac1 coding sequences are also in the Supplementary Experimental Procedures.

Deletion and transposon mutagenesis

Unmarked and non-polar deletions in *B. cenocepacia* K56-2 and J2315 strains, and in *B. multivorans* ATCC17616 were performed as described previously (Flannagan et al., 2008; Hamad et al., 2010). Random transposon mutagenesis in *B. cenocepacia* K56-2 Δ atsR was performed using the pTnMod-RTp' plasposon (Dennis and Zylstra, 1998). For further details, see the Supplementary Experimental Procedures.

Cell culture and transfection

293T cells and mouse BMDMs were cultured in DMEM (HyClone), while mouse DC2.4 dendritic cells were cultured in RPMI-1640. Details on culturing conditions and transfection are in the Supplementary Experimental Procedures.

Macrophage infections

To quantify the T6SS-dependent "beads on a string" phenotype (Aubert et al., 2015), infections were performed in the C57BL/6 murine bone marrow-derived macrophage cell line ANA-1 (Cox et al., 1989). Infection of DC2.4 dendritic cells and iBMDM cells was used to determine RhoA modification and inflammasome activation. Additional details are presented in Supplementary Experimental Procedures.

Hcp and TecA polyclonal antibodies and immunoblot analysis of TecA secretion

Hcp was PCR amplified and cloned into pET30a by use of NdeI and HindIII restriction sites, and introduced into *E. coli* strain BL21 (DE3) by transformation, generating pDA44. Hcp fused to 6xHis was purified and used to raise rabbit polyclonal antibodies. The peptide TRFNFETGDQWDGR from TecA was synthesized by ProSci Inc. (Poway, CA) and employed for rabbit immunization. See further details in Supplementary Experimental Procedures.

Inflammasome activation assays

Culture supernatants of primary BMDMs or EGFP-Pyrin-expressing DC2.4 cells that had been treated with indicated inflammasome stimuli were subjected to 15% trichloroacetic acid precipitation. Precipitates were analysed by anti-caspase-1 immunoblotting, and the total cell lysates were analyzed by anti- β -tubulin blotting as the loading control. IL-1 β secretion was measured using the IL-1 β ELISA kit (Neobioscience Technology Company). To determine pyroptotic cell death, the lactate dehydrogenase (LDH) assay was employed using the CytoTox 96 Non-Radioactive Cytotoxicity Assay kit (Promega).

Purification of recombinant proteins and *in vitro* deamidation reaction

His-tagged proteins were purified by affinity chromatography using Ni-NTA beads (Qiagen). For *in vitro* deamidation reaction, parental or mutant TecA recombinant proteins were incubated for 30 min at 37°C with RhoA (1:10 molar ratio) in a buffer made of 50 mM Tris-HCl (pH 7.5) and 150 mM NaCl. The resulting modified Rho proteins were subjected to mass spectrometry analyses directly or reaction with the C3

toxin. Approximately 0.1 µg of C3 toxin-reacted RhoA was separated on 15% SDS-PAGE gels followed by anti-RhoA immunoblotting. See further details in Supplementary Experimental Procedures.

Gel shift assay of RhoA ADP-ribosylation by the C3 toxin

DC2.4 or 293T cells were lysed by sonication in a buffer containing 20 mM Tris-HCl (pH 7.5), 150 mM NaCl, 20 mM β-OG and a protease inhibitor cocktail. The lysates were cleared by centrifugation at 16,000 g for 10 min. 15 µl of the supernatants were incubated with 1 µg of recombinant C3 toxin with NAD and thymidine for 15 min at 30 °C and the reaction was stopped by adding SDS sample buffer. Cells lysates were separated by SDS-PAGE in 15% SDS-polyacrylamide gels and analyzed by immunoblotting.

Mice infections

Cultures of *B. cenocepacia* J2315, *ΔtecA* or *ΔtecA* complemented with pTecA were used to infect C57BL/6 wild-type or *Mefv*^{-/-} mice intranasally to examine lung inflammation or intraperitoneally to investigate the lethal effect and bacteria loads. Lungs were removed for histopathology and sections stained with haematoxylin and eosin, and the damage of infected lungs was quantified by blindly scoring of the pathology. See further details in Supplementary Experimental Procedures. Animal experiments were conducted following the Ministry of Health national guidelines for housing and care of laboratory animals and performed in accordance with institutional regulations after review and approval by the Institutional Animal Care and Use Committee at National Institute of Biological Sciences.

479

480 **SUPPLEMENTAL INFORMATION**

481 Supplemental Information includes Supplementary Experimental Procedures,
482 Supplementary Figure 1 and Supplementary Table 1.

483

484 **AUTHOR CONTRIBUTIONS**

485 M.A.V. and F.S. conceived the study; D.F.A., H. X. and J.Y. performed the majority of
486 experiments; H.X. was assisted by W.G. X.S. performed mouse lethality and bacterial
487 load assays. L.L. and S.C. performed the mass spectrometry analyses. F.B. provided
488 technical assistance during the revision process. D.F.A., H. X., J.Y., M.A.V and F.S.
489 analyzed the data and wrote the manuscript. All authors discussed the results and
490 commented on the manuscript.

491

492 **ACKNOWLEDGEMENTS**

493 We thank members of the Shao laboratory for helpful discussions and technical
494 assistance. This work was supported by grants from Cystic Fibrosis Canada and the UK
495 Cystic Fibrosis Trust (to M.A.V) and grants from the Strategic Priority Research Program
496 of the Chinese Academy of Sciences (XDB08020202), the China National Science
497 Foundation Program for Distinguished Young Scholars (31225002), the Program for
498 International Collaborations (31461143006), and the National Basic Research Program of
499 China 973 Program (2012CB518700 and 2014CB849602) to F.S. M.A.V. was a Canada
500 Research Chair in Infectious Diseases and Microbial Pathogenesis. F.S. was also

501 supported in part by an International Early Career Scientist grant from the Howard
502 Hughes Medical Institute (55007431) and the Beijing Scholar Program.

503

504 REFERENCES

- 505 Abdulrahman, B.A., Khweek, A.A., Akhter, A., Caution, K., Kotrange, S., Abdelaziz,
506 D.H., Newland, C., Rosales-Reyes, R., Kopp, B., McCoy, K., *et al.* (2011). Autophagy
507 stimulation by rapamycin suppresses lung inflammation and infection by *Burkholderia*
508 *cenocepacia* in a model of cystic fibrosis. *Autophagy* 7, 1359-1370.
- 509 Aktories, K. (2011). Bacterial protein toxins that modify host regulatory GTPases. *Nat*
510 *Rev Microbiol* 9, 487-498.
- 511 Aubert, D., MacDonald, D.K., and Valvano, M.A. (2010). BcsKC is an essential protein
512 for the type VI secretion system activity in *Burkholderia cenocepacia* that forms an outer
513 membrane complex with BcsLB. *The Journal of biological chemistry* 285, 35988-35998.
- 514 Aubert, D.F., Flannagan, R.S., and Valvano, M.A. (2008). A novel sensor kinase-
515 response regulator hybrid controls biofilm formation and virulence in *Burkholderia*
516 *cenocepacia*. *Infect Immun* 76, 1979-1991.
- 517 Aubert, D.F., Hu, S., and Valvano, M.A. (2015). Quantification of Type VI secretion
518 system activity in macrophages infected with *Burkholderia cenocepacia*. *Microbiology*
519 *161*, 2161-2173.
- 520 Aubert, D.F., O'Grady, E.P., Hamad, M.A., Sokol, P.A., and Valvano, M.A. (2013). The
521 *Burkholderia cenocepacia* sensor kinase hybrid AtsR is a global regulator modulating
522 quorum-sensing signalling. *Environ Microbiol* 15, 372-385.
- 523 Basler, M., Pilhofer, M., Henderson, G.P., Jensen, G.J., and Mekalanos, J.J. (2012). Type
524 VI secretion requires a dynamic contractile phage tail-like structure. *Nature* 483, 182-
525 186.
- 526 Boyer, F., Fichant, G., Berthod, J., Vandenbrouck, Y., and Attree, I. (2009). Dissecting
527 the bacterial type VI secretion system by a genome wide in silico analysis: what can be
528 learned from available microbial genomic resources? *BMC Genomics* 10, 104.
- 529 Clemens, D.L., Ge, P., Lee, B.Y., Horwitz, M.A., and Zhou, Z.H. (2015). Atomic
530 structure of T6SS reveals interlaced array essential to function. *Cell* 160, 940-951.
- 531 Cox, G.W., Mathieson, B.J., Gandino, L., Blasi, E., Radzioch, D., and Varesio, L. (1989).
532 Heterogeneity of hematopoietic cells immortalized by v-myc/v-raf recombinant retrovirus
533 infection of bone marrow or fetal liver. *Journal of the National Cancer Institute* 81, 1492-
534 1496.
- 535 Cruz-Migoni, A., Hautbergue, G.M., Artymiuk, P.J., Baker, P.J., Bokori-Brown, M.,
536 Chang, C.T., Dickman, M.J., Essex-Lopresti, A., Harding, S.V., Mahadi, N.M., *et al.*
537 (2011). A *Burkholderia pseudomallei* toxin inhibits helicase activity of translation factor
538 eIF4A. *Science* 334, 821-824.

539 Cui, J., Yao, Q., Li, S., Ding, X., Lu, Q., Mao, H., Liu, L., Zheng, N., Chen, S., and Shao,
540 F. (2010). Glutamine deamidation and dysfunction of ubiquitin/NEDD8 induced by a
541 bacterial effector family. *Science* 329, 1215-1218.

542 Dennis, J.J., and Zylstra, G.J. (1998). Plasmids: modular self-cloning minitransposons
543 derivatives for rapid genetic analysis of gram-negative bacterial genomes. *Appl Environ*
544 *Microbiol* 64, 2710-2715.

545 Downey, D.G., Martin, S.L., Dempster, M., Moore, J.E., Keogan, M.T., Starcher, B.,
546 Edgar, J., Bilton, D., and Elborn, J.S. (2007). The relationship of clinical and
547 inflammatory markers to outcome in stable patients with cystic fibrosis. *Pediatric*
548 *pulmonology* 42, 216-220.

549 Drevinek, P., and Mahenthiralingam, E. (2010). *Burkholderia cenocepacia* in cystic
550 fibrosis: epidemiology and molecular mechanisms of virulence. *Clin Microbiol Infect* 16,
551 821-830.

552 Durand, E., Cambillau, C., Cascales, E., and Journet, L. (2014). VgrG, Tae, Tle, and
553 beyond: the versatile arsenal of Type VI secretion effectors. *Trends Microbiol* 22, 498-
554 507.

555 Durand, E., Derrez, E., Audoly, G., Spinelli, S., Ortiz-Lombardia, M., Raoult, D.,
556 Cascales, E., and Cambillau, C. (2012). Crystal structure of the VgrG1 actin cross-linking
557 domain of the *Vibrio cholerae* type VI secretion system. *The Journal of biological*
558 *chemistry* 287, 38190-38199.

559 Flannagan, R.S., Jaumouillé, V., Huynh, K.K., Plumb, J.D., Downey, G.P., Valvano,
560 M.A., and Grinstein, S. (2012). *Burkholderia cenocepacia* disrupts host cell actin
561 cytoskeleton by inactivating Rac and Cdc42. *Cell Microbiol* 14, 239-254.

562 Flannagan, R.S., Linn, T., and Valvano, M.A. (2008). A system for the construction of
563 targeted unmarked gene deletions in the genus *Burkholderia*. *Environ Microbiol* 10,
564 1652-1660.

565 Flatau, G., Landraud, L., Boquet, P., Bruzzone, M., and Munro, P. (2000). Deamidation
566 of RhoA glutamine 63 by the *Escherichia coli* CNF1 toxin requires a short sequence of
567 the GTPase switch 2 domain. *Biochem Biophys Res Commun* 267, 588-592.

568 Flatau, G., Lemichez, E., Gauthier, M., Chardin, P., Paris, S., Fiorentini, C., and Boquet,
569 P. (1997). Toxin-induced activation of the G protein p21 Rho by deamidation of
570 glutamine. *Nature* 387, 729-733.

571 Gavrilin, M.A., Abdelaziz, D.H., Mostafa, M., Abdulrahman, B.A., Grandhi, J., Akhter,
572 A., Abu Khweek, A., Aubert, D.F., Valvano, M.A., Wewers, M.D., *et al.* (2012).
573 Activation of the pyrin inflammasome by intracellular *Burkholderia cenocepacia*. *J*
574 *Immunol* 188, 3469-3477.

575 Hamad, M.A., Skeldon, A.M., and Valvano, M.A. (2010). Construction of
576 aminoglycoside-sensitive *Burkholderia cenocepacia* strains for use in studies of
577 intracellular bacteria with the gentamicin protection assay. *Appl Environ Microbiol* 76,
578 3170-3176.

579 Jiang, F., Waterfield, N.R., Yang, J., Yang, G., and Jin, Q. (2014). A *Pseudomonas*
580 *aeruginosa* Type VI Secretion Phospholipase D Effector Targets Both Prokaryotic and
581 Eukaryotic Cells. *Cell Host Microbe* 15, 600-610.

582 Keestra, A.M., Winter, M.G., Auburger, J.J., Frassle, S.P., Xavier, M.N., Winter, S.E.,
583 Kim, A., Poon, V., Ravesloot, M.M., Waldenmaier, J.F., *et al.* (2013). Manipulation of
584 small Rho GTPases is a pathogen-induced process detected by NOD1. *Nature* 496, 233-
585 237.

586 Keith, K.E., Hynes, D.W., Sholdice, J.E., and Valvano, M.A. (2009). Delayed association
587 of the NADPH oxidase complex with macrophage vacuoles containing the opportunistic
588 pathogen *Burkholderia cenocepacia*. *Microbiology* 155, 1004-1015.

589 Khodai-Kalaki, M., Andrade, A., Fathy Mohamed, Y., and Valvano, M.A. (2015).
590 *Burkholderia cenocepacia* Lipopolysaccharide Modification and Flagellin Glycosylation
591 Affect Virulence but Not Innate Immune Recognition in Plants. *MBio* 6, e00679.

592 Khodai-Kalaki, M., Aubert, D.F., and Valvano, M.A. (2013). Characterization of the
593 AtsR hybrid sensor kinase phosphorelay pathway and identification of its response
594 regulator in *Burkholderia cenocepacia*. *The Journal of biological chemistry* 288, 30473-
595 30484.

596 Kopp, B.T., Abdulrahman, B.A., Khweek, A.A., Kumar, S.B., Akhter, A., Montione, R.,
597 Tazi, M.F., Caution, K., McCoy, K., and Amer, A.O. (2012). Exaggerated inflammatory
598 responses mediated by *Burkholderia cenocepacia* in human macrophages derived from
599 Cystic fibrosis patients. *Biochem Biophys Res Commun* 424, 221-227.

600 Kudryashev, M., Wang, R.Y., Brackmann, M., Scherer, S., Maier, T., Baker, D., DiMaio,
601 F., Stahlberg, H., Egelman, E.H., and Basler, M. (2015). Structure of the type VI
602 secretion system contractile sheath. *Cell* 160, 952-962.

603 Lockman, H.A., Gillespie, R.A., Baker, B.D., and Shakhnovich, E. (2002). *Yersinia*
604 *pseudotuberculosis* produces a cytotoxic necrotizing factor. *Infect Immun* 70, 2708-2714.

605 Mahenthiralingam, E., Coenye, T., Chung, J.W., Speert, D.P., Govan, J.R., Taylor, P.,
606 and Vandamme, P. (2000). Diagnostically and experimentally useful panel of strains
607 from the *Burkholderia cepacia* complex. *J Clin Microbiol* 38, 910-913.

608 Mansfield, E., Chae, J.J., Komarow, H.D., Brotz, T.M., Frucht, D.M., Aksentijevich, I.,
609 and Kastner, D.L. (2001). The familial Mediterranean fever protein, pyrin, associates
610 with microtubules and colocalizes with actin filaments. *Blood* 98, 851-859.

611 Miyata, S.T., Kitaoka, M., Brooks, T.M., McAuley, S.B., and Pukatzki, S. (2011). *Vibrio*
612 *cholerae* requires the type VI secretion system virulence factor VasX to kill
613 *Dictyostelium discoideum*. *Infect Immun* 79, 2941-2949.

614 Miyata, S.T., Unterweger, D., Rudko, S.P., and Pukatzki, S. (2013). Dual expression
615 profile of type VI secretion system immunity genes protects pandemic *Vibrio cholerae*.
616 *PLoS Pathog* 9, e1003752.

617 Ortega, X., Hunt, T.A., Loutet, S., Vinion-Dubiel, A.D., Datta, A., Choudhury, B.,
618 Goldberg, J.B., Carlson, R., and Valvano, M.A. (2005). Reconstitution of O-specific
619 lipopolysaccharide expression in the *Burkholderia cenocepacia* strain J2315 that is
620 associated with transmissible infections in patients with cystic fibrosis. *J Bacteriol* 187,
621 1324-1333.

622 Orth, J.H., Preuss, I., Fester, I., Schlosser, A., Wilson, B.A., and Aktories, K. (2009).
623 *Pasteurella multocida* toxin activation of heterotrimeric G proteins by deamidation. *Proc*
624 *Natl Acad Sci U S A* 106, 7179-7184.

625 Rosales-Reyes, R., Skeldon, A.M., Aubert, D.F., and Valvano, M.A. (2012). The Type
626 VI secretion system of *Burkholderia cenocepacia* targets multiple Rho family GTPases
627 disrupting the actin cytoskeleton and the assembly of NADPH oxidase complex in
628 macrophages. *Cell Microbiol* 14, 255-273.

629 Roy, A., Kucukural, A., and Zhang, Y. (2010). I-TASSER: a unified platform for
630 automated protein structure and function prediction. *Nat Protoc* 5, 725-738.

631 Russell, A.B., Peterson, S.B., and Mougous, J.D. (2014). Type VI secretion system
632 effectors: poisons with a purpose. *Nat Rev Microbiol* 12, 137-148.

633 Saldías, M.S., Ortega, X., and Valvano, M.A. (2009). *Burkholderia cenocepacia* O
634 antigen lipopolysaccharide prevents phagocytosis by macrophages and adhesion to
635 epithelial cells. *Journal of medical microbiology* 58, 1542-1548.

636 Sana, T.G., Baumann, C., Merdes, A., Soscia, C., Rattei, T., Hachani, A., Jones, C.,
637 Bennett, K.L., Filloux, A., Superti-Furga, G., *et al.* (2015). Internalization of
638 *Pseudomonas aeruginosa* Strain PAO1 into Epithelial Cells Is Promoted by Interaction of
639 a T6SS Effector with the Microtubule Network. *MBio* 6, e00712.

640 Sanada, T., Kim, M., Mimuro, H., Suzuki, M., Ogawa, M., Oyama, A., Ashida, H.,
641 Kobayashi, T., Koyama, T., Nagai, S., *et al.* (2012). The *Shigella flexneri* effector OspI
642 deamidates UBC13 to dampen the inflammatory response. *Nature* 483, 623-626.

643 Schmerk, C.L., and Valvano, M.A. (2013). *Burkholderia multivorans* survival and
644 trafficking within macrophages. *J Med Microbiol* 62, 173-184.

645 Schmidt, G., Sehr, P., Wilm, M., Selzer, J., Mann, M., and Aktories, K. (1997). Gln 63 of
646 Rho is deamidated by *Escherichia coli* cytotoxic necrotizing factor-1. *Nature* 387, 725-
647 729.

648 Schwab, U., Abdullah, L.H., Perlmutter, O.S., Albert, D., Davis, C.W., Arnold, R.R.,
649 Yankaskas, J.R., Gilligan, P., Neubauer, H., Randell, S.H., *et al.* (2014). Localization of
650 *Burkholderia cepacia* complex bacteria in cystic fibrosis lungs and interactions with
651 *Pseudomonas aeruginosa* in hypoxic mucus. *Infect Immun* 82, 4729-4745.

652 Schwarz, S., Singh, P., Robertson, J.D., LeRoux, M., Skerrett, S.J., Goodlett, D.R., West,
653 T.E., and Mougous, J.D. (2014). VgrG-5 is a *Burkholderia* type VI secretion system-
654 exported protein required for multinucleated giant cell formation and virulence. *Infect*
655 *Immun* 82, 1445-1452.

656 Suarez, G., Sierra, J.C., Erova, T.E., Sha, J., Horneman, A.J., and Chopra, A.K. (2010). A
657 type VI secretion system effector protein, VgrG1, from *Aeromonas hydrophila* that
658 induces host cell toxicity by ADP ribosylation of actin. *J Bacteriol* 192, 155-168.

659 Toesca, I.J., French, C.T., and Miller, J.F. (2014). The Type VI secretion system spike
660 protein VgrG5 mediates membrane fusion during intercellular spread by pseudomallei
661 group *Burkholderia* species. *Infect Immun* 82, 1436-1444.

662 Uehlinger, S., Schwager, S., Bernier, S.P., Riedel, K., Nguyen, D.T., Sokol, P.A., and
663 Eberl, L. (2009). Identification of specific and universal virulence factors in *Burkholderia*
664 *cenocepacia* strains by using multiple infection hosts. *Infect Immun* 77, 4102-4110.

665 Valvano, M.A., Rosales-Reyes, R., Schmerk, C.L., and Ostapska, H. (2012). Molecular
666 mechanisms of virulence of *Burkholderia cepacia* complex bacteria. In *Burkholderia:*
667 *From Genomes to Function*, T. Coeyne, and E. Mahenthiralingam, eds. (Norfolk, UK.,
668 Caister Academic Press), pp. 149-160.

669 Vergunst, A.C., Meijer, A.H., Renshaw, S.A., and O'Callaghan, D. (2010). *Burkholderia*
670 *cenocepacia* creates an intramacrophage replication niche in zebrafish embryos, followed
671 by bacterial dissemination and establishment of systemic infection. *Infect Immun* 78,
672 1495-1508.

673 Waite, A.L., Schaner, P., Hu, C., Richards, N., Balci-Peynircioglu, B., Hong, A., Fox,
674 M., and Gumucio, D.L. (2009). Pyrin and ASC co-localize to cellular sites that are rich in
675 polymerizing actin. *Experimental biology and medicine* 234, 40-52.

676 Washington, E.J., Banfield, M.J., and Dangel, J.L. (2013). What a difference a Dalton
677 makes: bacterial virulence factors modulate eukaryotic host cell signaling systems via
678 deamidation. *Microbiology and molecular biology reviews : MMBR* 77, 527-539.

679 Xu, H., Yang, J., Gao, W., Li, L., Li, P., Zhang, L., Gong, Y.N., Peng, X., Xi, J.J., Chen,
680 S., *et al.* (2014). Innate immune sensing of bacterial modifications of Rho GTPases by
681 the Pyrin inflammasome. *Nature* 513, 237-241.

682 Yang, J., Xu, H., and Shao, F. (2014). The immunological function of familial
683 Mediterranean fever disease protein Pyrin. *Science China Life sciences* 57, 1156-1161.

684 Yao, Q., Cui, J., Wang, J., Li, T., Wan, X., Luo, T., Gong, Y.N., Xu, Y., Huang, N., and
685 Shao, F. (2012). Structural mechanism of ubiquitin and NEDD8 deamidation catalyzed
686 by bacterial effectors that induce macrophage-specific apoptosis. *Proc Natl Acad Sci U S*
687 *A 109*, 20395-20400.

688 Yu, Y., Fang, L., Zhang, Y., Sheng, H., and Fang, W. (2015). VgrG2 of type VI secretion
689 system 2 of *Vibrio parahaemolyticus* induces autophagy in macrophages. *Frontiers in*
690 *microbiology 6*, 168.

691 Zhang, L., Krachler, A.M., Broberg, C.A., Li, Y., Mirzaei, H., Gilpin, C.J., and Orth, K.
692 (2012). Type III effector VopC mediates invasion for *Vibrio* species. *Cell reports 1*, 453-
693 460.

694 Zheng, J., and Leung, K.Y. (2007). Dissection of a type VI secretion system in
695 *Edwardsiella tarda*. *Mol Microbiol 66*, 1192-1206.

696 Zoued, A., Brunet, Y.R., Durand, E., Aschtgen, M.S., Logger, L., Douzi, B., Journet, L.,
697 Cambillau, C., and Cascales, E. (2014). Architecture and assembly of the Type VI
698 secretion system. *Biochim Biophys Acta 1843*, 1664-1673.
699
700
701

FIGURE LEGENDS

Figure 1. Identification of *tecA* Encoding A Novel Non-VgrG T6SS Effector Functioning in Eukaryotic Host Cells.

(A) Genetic map of the *B. cenocepacia* K56-2 T6SS gene cluster located on chromosome 1 (Chr. 1) and the *tecA* (BCAM1857) region on chromosome 2 (Chr. 2). Arrows indicate direction of transcription of each gene. Genes outside the T6SS cluster are indicated in black. *hcp* and *tecA* are highlighted in red. White circles indicate the position of the transposon insertion.

(B) Phase-contrast microscopy of ANA-1 macrophages at 4 h post-infection (MOI of 50) with *B. cenocepacia* K56-2 Δ *atsR* and Δ *atsR* Δ *tecA* carrying the vector control pDA12 or complementing plasmid pTecA. The arrows indicate “beads on a string”-like structures.

(C) Quantification of the development of “beads on a string”-like structures in *B. cenocepacia*-infected ANA-1 macrophages. Results were expressed in arbitrary units relative to Δ *atsR* set as 1. Values are mean \pm standard deviation from at least 21 fields of view, and representative of three independent experiments. Cells infected with *B. cenocepacia* K56-2 Δ *atsR* Δ *hcp* were used as negative control.

(D) Phase-contrast microscopy of ANA-1 macrophages infected with *B. multivorans* Δ *atsR*_{Bm} using the same conditions as in (B). The arrows mark the “beads on a string”-like structures.

See also Figure S1.

Figure 2. A T6SS-dependent Activity in *B. cenocepacia* That Leads to Rho Deamidation.

725 (A) T6SS-dependent Asn-41 deamidation of RhoA during *B. cenocepacia* infection.
726 FLAG-RhoA was stably expressed and purified from DC2.4 cells infected with *B.*
727 *cenocepacia* J2315 or its Δhcp mutant, and analysed by mass spectrometry. The upper
728 panel shows the extracted ion chromatograms of the Asn-41-containing peptide. The
729 lower panel shows the behavior of endogenous RhoA in response to further modification
730 by the C3 toxin.

731 (B) RhoA modification by cytosolic extracts of *B. cenocepacia*-infected cells. RhoA
732 purified from non-infected DC2.4 cells was incubated with cytosolic extracts of DC2.4
733 cells infected with J2315 or Δhcp , and then subjected to further *in vitro* modification by
734 the C3 toxin. Anti-tubulin immunoblot serves as the loading control.

735 (C) Reconstitution of RhoA modification by bacteria-containing pellets of J2315-infected
736 cell lysates. Pellets of lysates of DC2.4 cells infected with J2315 or Δhcp were used as
737 the source of activity to modify RhoA from non-infected DC2.4 cells. RhoA was
738 subjected to further *in vitro* modification by the C3 toxin. Anti-tubulin immunoblot
739 serves as the loading control.

740 (D) RhoA modification by lysates of J2315 but not *E. coli* and *B. thailandensis* (*B.t.*).
741 RhoA from non-infected DC2.4 cells was incubated with the indicated bacterial lysates
742 and subjected to further *in vitro* modification by the C3 toxin. Anti-tubulin immunoblot
743 serves as the loading control.

744 (E) Asn-41 deamidation of RhoA in J2315 but not *E. coli*. WT or the N41A mutant RhoA
745 was recombinantly expressed and purified from *B. cenocepacia* (WT or $\Delta tecA$) or *E. coli*.
746 The purified RhoA was subjected to further *in vitro* modification by the C3 toxin (upper)
747 or mass spectrometry analyses. The lower panel shows the extracted ion chromatograms

of the Asn-41-containing peptide of RhoA from *B. cenocepacia* (*B.c.*) and *E. coli*.
Spectrum 1/2 and 3/4 are from two separate experiments.

Figure 3. TecA Induces Rho Deamidation in Various Cellular Systems and Causes Actin Cytoskeleton Disruption.

(A and B) Modification of endogenous RhoA by TecA during *B. cenocepacia* infection. DC2.4 cells were infected with J2315 or the indicated mutant strains. Cell lysates were subjected to *in vitro* modification by the C3 toxin followed by immunoblotting analyses.

An empty vector (Vec) or a plasmid expressing TecA was introduced into $\Delta tecA$ in (B).

(C) Ectopic expression of TecA in *B. thailandensis* induces endogenous RhoA modification during infection. DC2.4 cells were infected with *B. thailandensis* harboring an empty vector (Vec) or a TecA-expressing plasmid, or *B. cenocepacia* J2315 as a control. Assay of RhoA modification was performed similarly as that in (A). C41A is a catalytic cysteine mutant of TecA.

(D and E) Asn-41 deamidation of RhoA by TecA in transfected 293T cells. 293T cells were transfected with Myc-tagged TecA (WT or the C41A mutant). Endogenous RhoA modification in (D) was detected as in (A). In (E), cells were co-transfected with FLAG-RhoA and purified FLAG-RhoA was subjected to mass spectrometry analyses; shown are extracted ion chromatograms of the Asn-41-containing peptide.

(F) Asn-41 deamidation of RhoA by TecA co-expressed in *E. coli*. *E. coli* BL21 strain was transformed with two plasmids expressing His-RhoA and TecA (WT or the C41A mutant). Purified His-RhoA was subjected to mass spectrometry analyses and shown are extracted ion chromatograms of the Asn-41-containing peptide.

(G) Asn-39 deamidation of Rac1 by TecA in 293T cells. 293T cells were co-transfected with FLAG-Rac1 and Myc-TecA (WT or the C41A mutant). FLAG-Rac1 deamidation was assayed by mass spectrometry and extracted ion chromatograms of the Asn-39-containing peptide are shown.

(H) Deamidated Rac1 mimics TecA to alter the actin cytoskeleton structure. 293T cells were transfected with RhoA N41D or Rac1 N39D mutant together with EGFP as the transfection marker. Shown are the confocal fluorescence images of representative transfected cells. The arrows indicate “beads on a string”-like structures.

Figure 4. The TecA Family of Bacterial Proteins with Putative Cysteine Protease-like Fold and Catalytic Triad.

(A) ClustalW analysis of TecA orthologs ordered based on their sequence identity to TecA of *B. cenocepacia* K56-2 (which is 100% identical to TecA of J2315). TecA orthologs are present in *B. cenocepacia* (*B. ceno*), *B. contaminans* (*B. cont*), *B. pyrrocinia* (*B. pyrr*), *B. lata*, *B. cepacia* ATCC25416 (*B. cep*), *B. ubonensis* (*B. ubo*), *Alcaligenes faecalis*, *Chryseobacterium indologenes*, *Flavobacterium branchiophilum*, and *Ochrobactrum anthropi*. Conserved residues are depicted in red. Asterisks indicate the putative Cys-His-Asp catalytic triad residues.

(B) *In silico* predicted structural model of *B. cenocepacia* K56-2 TecA, showing the location of the critical Cys-41 and His-105 residues of the putative catalytic triad. The Asp-148 is in a predicted unstructured region and therefore not indicated in the model.

Figure 5. TecA and Its Homologs Can Deamidate Rho GTPases *In Vitro*.

(A) Putative Cys-His-Asp catalytic triad residues are important for TecA modification of RhoA. 293T cells were transfected with Myc-TecA (WT or indicated mutants). Cell lysates were subjected to *in vitro* modification by the C3 toxin followed by immunoblotting. ΔC20 lacks the C-terminal 20 residues of TecA.

(B) RhoA modification by TecA homologs in 293T cells. 293T cells were transfected with mammalian expression plasmids encoding WP_034735953 (*C. indologenes*), WP_014085254 (*F. branchiophilum*) or WP_011982319 (*O. anthropi*). Cell lysates were subjected to *in vitro* modification by the C3 toxin followed by immunoblotting.

(C and D) Recombinant WP_034735953 from *C. indologenes* deamidates RhoA and Rac1 *in vitro*. Recombinant His-tagged WP_034735953 (WT or the catalytic cysteine mutant C40A) was incubated with purified RhoA or Rac1. Assay of RhoA modification by the C3 toxin in (C) was similar to that in (A). RhoA and Rac1 after incubation were analyzed by mass spectrometry. Shown in (D) are the extracted ion chromatograms of the peptide containing Asn-41 (for RhoA) or Asn-39 (for Rac1).

Figure 6. TecA Deamidation of RhoA Mediates *B. cenocepacia*-induced Pyrin Inflammasome Activation.

(A-D) TecA mediates *B. cenocepacia* infection-induced Pyrin inflammasome activation in its deamidase activity-dependent manner in mouse macrophages. Primary bone marrow-derived macrophage (BMDM) cells derived from WT (C57BL/6) or *Mefv*^{-/-} mice were infected with wild-type *B. cenocepacia* J2315 or its Δ*tecA* mutant or stimulated with LPS plus nigericin (Nig) as a control. Cell supernatants were examined by immunoblotting with anti-caspase-1 in (A and C) (immunoblotting of tubulin in the cell

lysates serves as a loading control). Pro-Casp1, caspase-1 precursor; p10, the mature caspase-1. ELISA of IL-1 β release and pyroptotic cell death measured by LDH release (n=3; mean \pm SD) are shown in (B and D). In (C and D), $\Delta tecA$ was complemented with a plasmid expressing WT TecA or the indicated catalytic mutants.

(E) TecA mediates *B. cenocepacia* infection-induced Pyrin inflammasome activation in DC2.4 cells. DC2.4 cells stably expressing Pyrin were infected with *B. cenocepacia* J2315 or the indicated mutant and complementation strains similarly as in (A and C). Cell supernatants were examined by anti-caspase-1 immunoblotting; immunoblotting of tubulin in the cell lysates serves as a loading control. Pro-Casp1, caspase-1 precursor; p10, the mature caspase-1.

(F) A deamidation-resistant mutant RhoA inhibits *B. cenocepacia*-induced Pyrin inflammasome activation. DC 2.4 cells stably expressing FLAG-tagged wild-type RhoA or the denoted N/L mutant of RhoA, Rac1 or Cdc42 were infected with *B. cenocepacia* J2315. The supernatant were subjected to anti-caspase-1 immunoblotting. Immunoblotting of tubulin in cell lysates serves as a loading control. Anti-FLAG immunoblot in the lower panel shows the expression of exogenous Rho GTPases. Pro-Casp1, caspase-1 precursor; p20, the mature caspase-1.

Figure 7. The Rho Deamidase Activity of TecA Triggers Inflammation and Its Recognition by Pyrin Protects Mice from Lethal *B. cenocepacia* Infection.

(A and B) WT C57BL/6 mice were infected with *B. cenocepacia* J2315 wild-type strain, or $\Delta tecA$, or $\Delta tecA$ containing a plasmid expressing TecA (WT or the C41A mutant). Representative haematoxylin & eosin staining of the lung sections is shown in (A).

840 Quantification scores of the lung injury ((n=2; mean \pm SD) are shown in (B). Data shown
841 are representative of two independent repetitions.

842 (C) Survival of mice (WT and *Mefv*^{-/-}) following peritoneal infection of *B. cenocepacia*
843 J2315 (wild-type or the $\Delta tecA$ strain). Survival curve analysis was performed with the
844 log-rank (Mantel–Cox) test in GraphPad Prism 5 (*P \leq 0.05). Data shown are
845 representative of three independent experiments.

846 (D) Bacterial loads in the spleen and liver of mice intraperitoneally infected with *B.*
847 *cenocepacia* J2315 (wild-type or the $\Delta tecA$ strain). Colony-forming units (CFUs) per
848 gram of tissues 4 days after infection are shown as mean values (n=7). *P \leq 0.05; ns,
849 non-significant (two-tailed unpaired Student's *t*-test).

Figure 1. Identification of *tecA* Encoding A Novel Non-VgrG T6SS Effector Functioning in Eukaryotic Host Cells

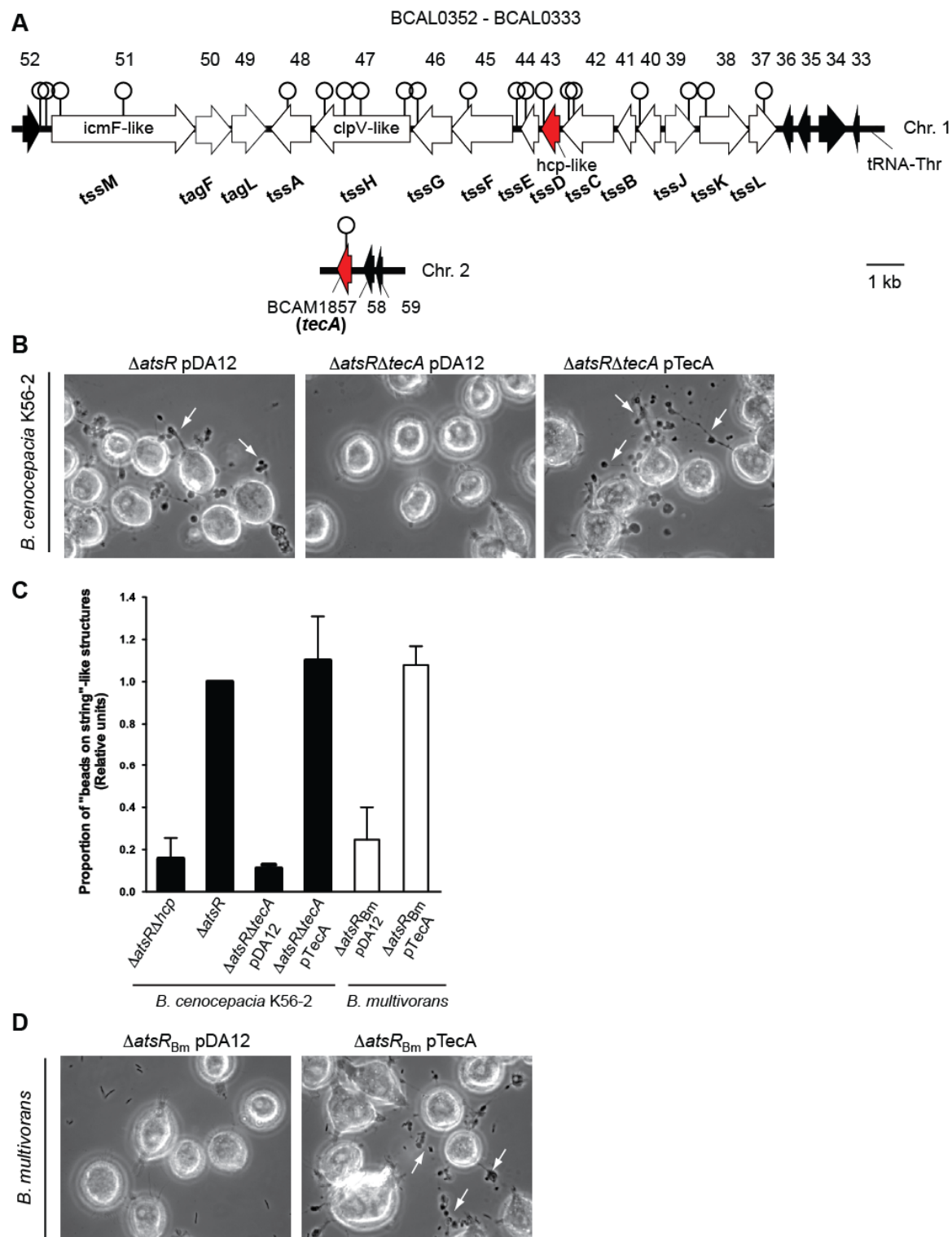


Figure 2. A T6SS-dependent Activity in *B. cenocepacia* That Leads to Rho Deamidation

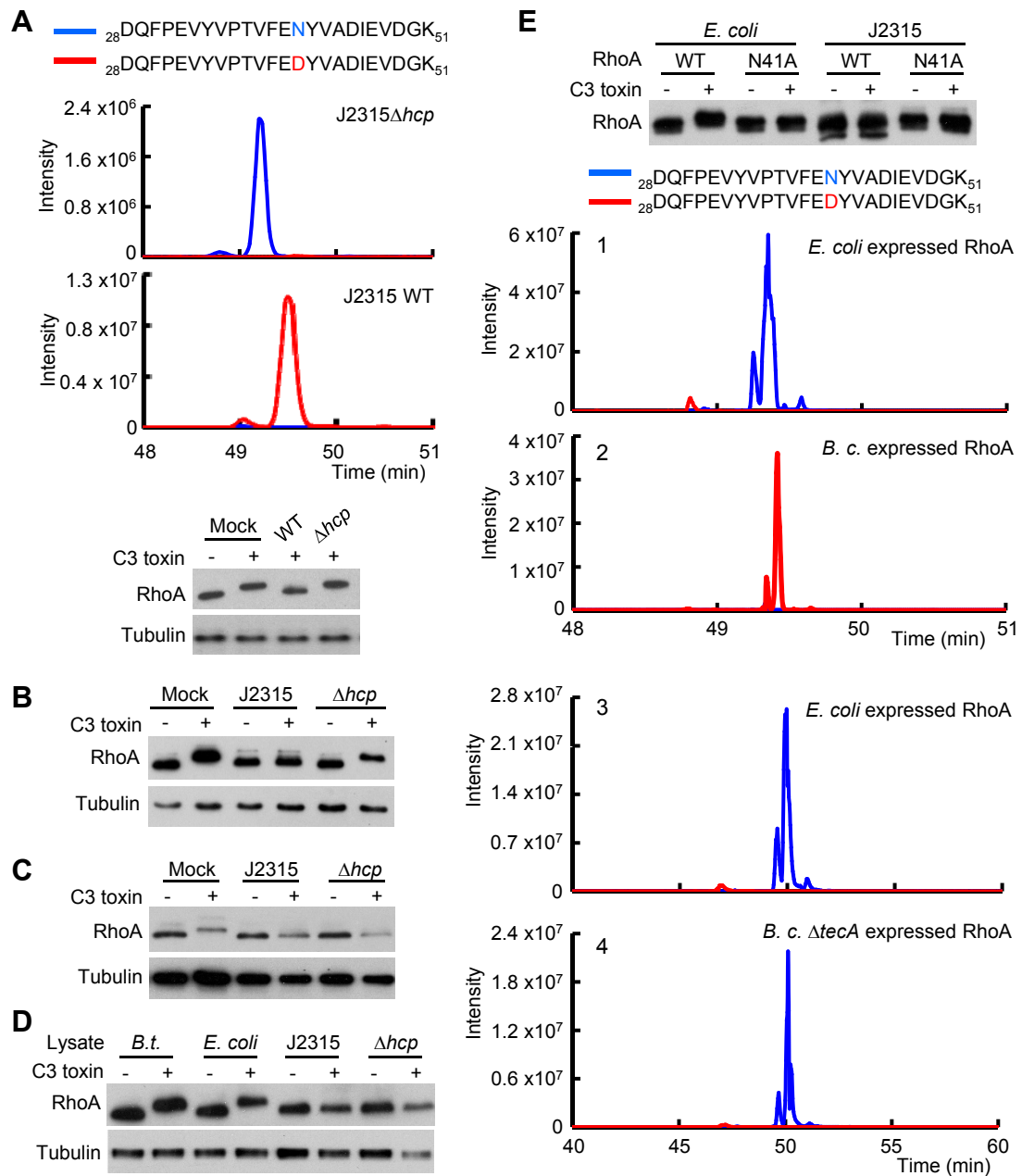


Figure 3. TecA Induces Rho Deamidation in Various Cellular Systems and Causes Actin Cytoskeleton Disruption

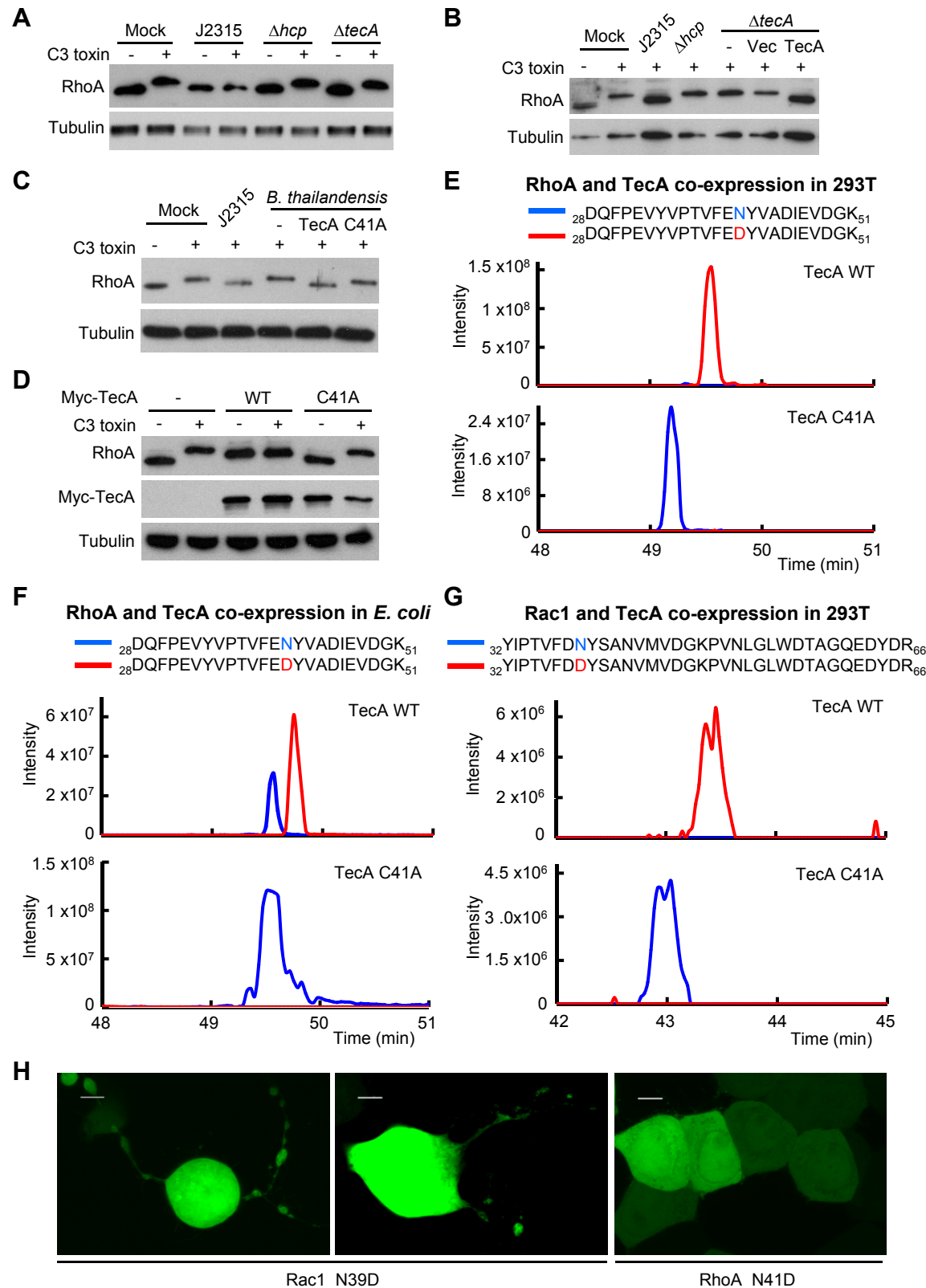


Figure 4. The TecA Family of Bacterial Proteins with Putative Cysteine
Protease-like Fold and Catalytic Triad

A

TecA (B. ceno K-56-2)	100%	---MQLTQLGGHVAQSGIAERQKH-AQALMF GMA --NID EY VS RGV CYDAAAYVRYLLRADAL IAPDALLD TA GS W RT RFNFET
I35_5735 (B ceno H111)	99%	---MQLTQLGGHVAQSGIAERQKH-AQALMF GMA --NID EY VS RGV CYDAAAYVRYLLRADAL IAPDALLD TA GS W RT RFNFET
ABF78545 (B ceno AU1054)	91%	---MQLTQLGGHVAQSGIAERQKH-AQALMF GMA --NID EY VS GGV CYDAAAYVRYLLRADAM IAPGTL LD TI GS W RT RF NFET
ABK11448 (B ceno HI2424)	91%	---MQLTQLGGHVAQSGIAERQKH-AQALMF GMA --NID EY VS GGV CYDAAAYVRYLLRADAM IAPGTL LD TI GS W RT RF NFET
ACA94711 (B ceno MC0-3)	91%	---MQLTQLGGHVAQSGIAERQKH-AQALMF GMA --NID EY VS GGV CYDAAAYVRYLLRADAM IAPGTL LD TI GS W RT RF NFET
AKM38892 (B cont)	85%	---MQLS QL GGHVAQSGFAERQKH-AQALMF GMA --DINEYVS GGV CYDAAAYVRYLLRSDAM IAPGALLD TI GS W RT RFNFET
WP_034180375 (B pyr)	84%	---MQLTQLGGHVAQSGFAEKQKH-AQALMY GMA --DINEYVS GGV CYDAAAYVRYLLRSDAM IAPDML LD TI GS W RT RF NFET
KML42510 (B lata)	85%	---MQLS QL GGHVAQSGFAERQKH-AQALMF GMA --DINEYVS GGV CYDAAAYVRYLLRSDAM IAPGALLD TI GS W RT RFNFET
AIO30069 (B cep ATCC 25416)	85%	---MQLS QL GGHVAQSGFAERQKH-AQALMF GMA --DINEYVS GGV CYDAAAYVRYLLRSDAM IAPGALLD TI GS W RT RFNFET
EAY64595 (B ceno PC184)	83%	---MQLS QL GGHVAQSGFAERQKH-AQALMF GMS --NID EY VS GGV CYDAAAYVRYLLRADAM IAPGTL LD TI GS W RT RF NFET
WP_010098838 (B ubo)	78%	---MELTQLGSQVAFQFAERQKH-AQALMY GMA --NITEYVPRGV CYDAAAF VRYLLQGHGLITPGVLLD TT GN WR PRPFNEA
WP_026483358 (A faecalis)	50%	---MNLTEKGTAKLSASDRIIYADN LH IGPD--DITAYM-KGV CYDAAAY MRYLLYNAK--IS FD RLLTSIS Q N W LPVVFKEA
WP_034735953 (C indologenes)	42%	---MSLTPEGATKALGPSE RA TV-ANALLAG FE --NIS KY N-TGVCHDVVAY TY LMRGAS--IS PN DLSEL T GS W LRKFDYMG
WP_014085254 (F branchiophilum)	38%	---MSVINPLGALEAKKSSVARS DI -GYKLLT GE --NIS RY N-SGICH DV VAY TY LM GS H--IS PN ELVQNK G EW L DKFNYLG
WP_011982319 (O anthropi)	37%	MEVLMH LT GYGENFIRSDRSTLFR GN L L AAGSE DN YITVDLSEAG CYDAAV LRFL FG AG--IS LN TLRG TS SS Q N W IPILN FR A

TecA (B. ceno K-56-2)	100%	GDQWDGRASIPAGTAVGFAR--GGNVF HAA IAVG-GTRIRAIN GGL L GAG WMNPVDLARALQ---PDPAGGFTYDRTTIRVHLSRL
I35_5735 (B ceno H111)	99%	GDQWDGRASIPAGTAVGFAR--GGNVF HAA IAVG-GTRIRAIN GGL L GAG WMNPVDLARALQ---PDPAGGFTYDRTTIRVHLSRL
ABF78545 (B ceno AU1054)	91%	GNQWDGRASIPAGTAVGFAR--GTNVF HAA IAVG-GTRIRGIN GGL L GAG WLHPVDLARVLQ---PDPAGGFAYDRTTIRVYLSRL
ABK11448 (B ceno HI2424)	91%	GNQWDGRASIPAGTAVGFAR--GTNVF HAA IAVG-GTRIRGIN GGL L GAG WLHPVDLARVLQ---PDPAGGFAYDRTTIRVYLSRL
ACA94711 (B ceno MC0-3)	91%	GNQWDGRASIPAGTAVGFAR--GTNVF HAA IAVG-GTRIRGIN GGL L GAG WLHPVDLARVLQ---PDPAGGFAYDRTTIRVYLSRL
AKM38892 (B cont)	85%	GGQWDGRASIPAGTAVGFSR--GGTVF HAA IAVG-GSRIRAIN GGR L GSG WMYA VD LARVLE---PDAAGGFTYDRANIRVHLSRL
WP_034180375 (B pyr)	84%	GDQWDGRASIPAGTAVGFSR--GGNVF HAA IAVG-GSRIRAIN GGR L GSG WMYA VD LARVLE---QDAAGGFTYDRANIRVHLSRL
KML42510 (B lata)	85%	GGQWDGRASIPAGTAVGFSR--GGTVF HAA IAVG-GSRIRAIN GGR L GSG WMYA VD LARVLE---PDAAGGFTYDRANIRVHLSRL
AIO30069 (B cep ATCC 25416)	85%	GGQWDGRASIPAGTAVGFSR--GGTVF HAA IAVG-GSRIRAIN GGR L GSG WMYA VD LARVLE---PDAAGGFTYDRANIRVHLSRL
EAY64595 (B ceno PC184)	83%	GNQWDGRASIPAGTAVGFAR--GTNVF HAA IAVG-GTRIRGIN GGL V GAG WLHPVDLARVLQ---PDPAGGFAYDRTTIRVYLSRL
WP_010098838 (B ubo)	78%	GNQWDGRASIPAGTAVGFSR--GGNVF HAA IAVG-GTRIRAVN GGR L GSG WL YP VDLARVLA---RQDDGAFLYDRTNIRVHLSRL
WP_026483358 (A faecalis)	50%	GRMWDGRNSLP GG K AI G FC RVKME FF HAAVAVG-GTEIRAIN GGL L GAG WLHPVDLARVLT--QKNEDG S FKYD G TDIFVYISNL
WP_034735953 (C indologenes)	42%	GEKWDGYSVLP KG K AI G FY RLIDK TF FHSAIT T ENIDYARSVN GK L G V G WDRPVD FK WE L G--KKNEDG T FN Y DG T KIEVYISL
WP_014085254 (F branchiophilum)	38%	GKKWDGTFFLD RG K AI G FY RLIDK TF FHSAIT T EN G TEIRSVN GH S L GT W LVPSNLS-CLG--ARD DD G T YR Y DG T KIEVYISL
WP_011982319 (O anthropi)	37%	GEQWNGYSAL FF G K A I G FY VD Q AG HI F HA PISL G -DV HI RG VH G K L G Q N WQDRINLT EV LPYSSRN PD G S FN Y DR R K II YVYISL

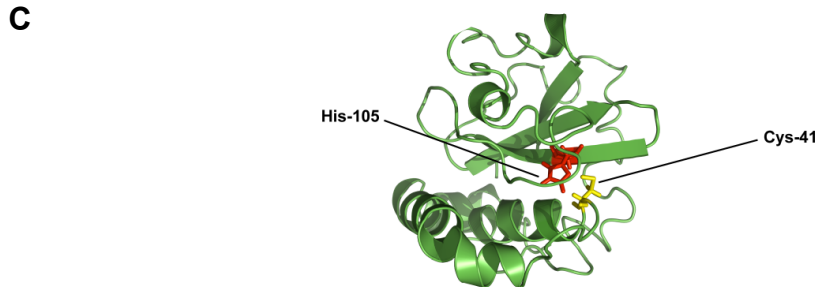


Figure 5. TecA and Its Homologs Can Deamidate Rho GTPases *In Vitro*

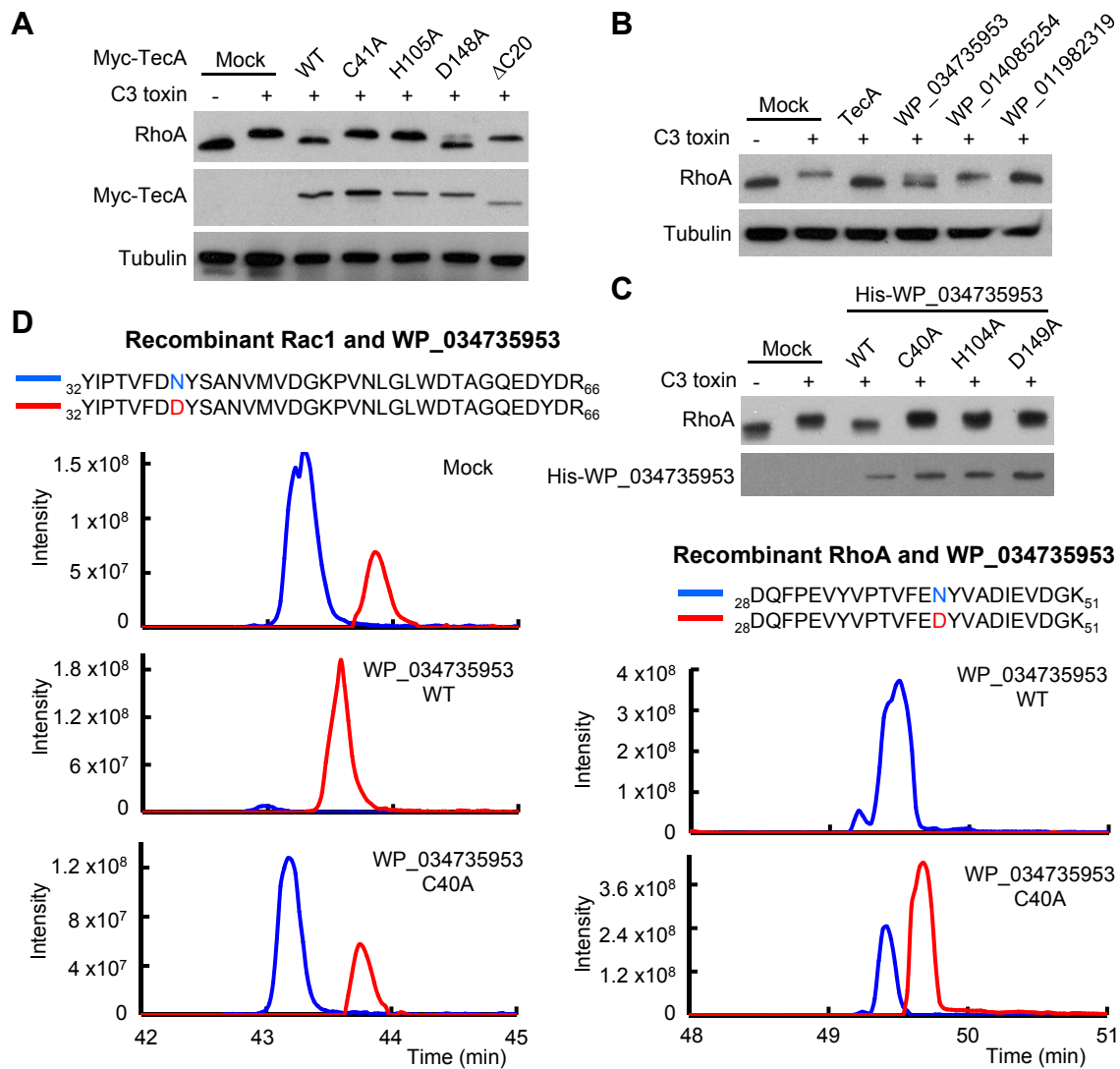


Figure 6. TecA Deamidation of RhoA Mediates *B. cenocepacia*-induced Pyrin Inflammasome Activation

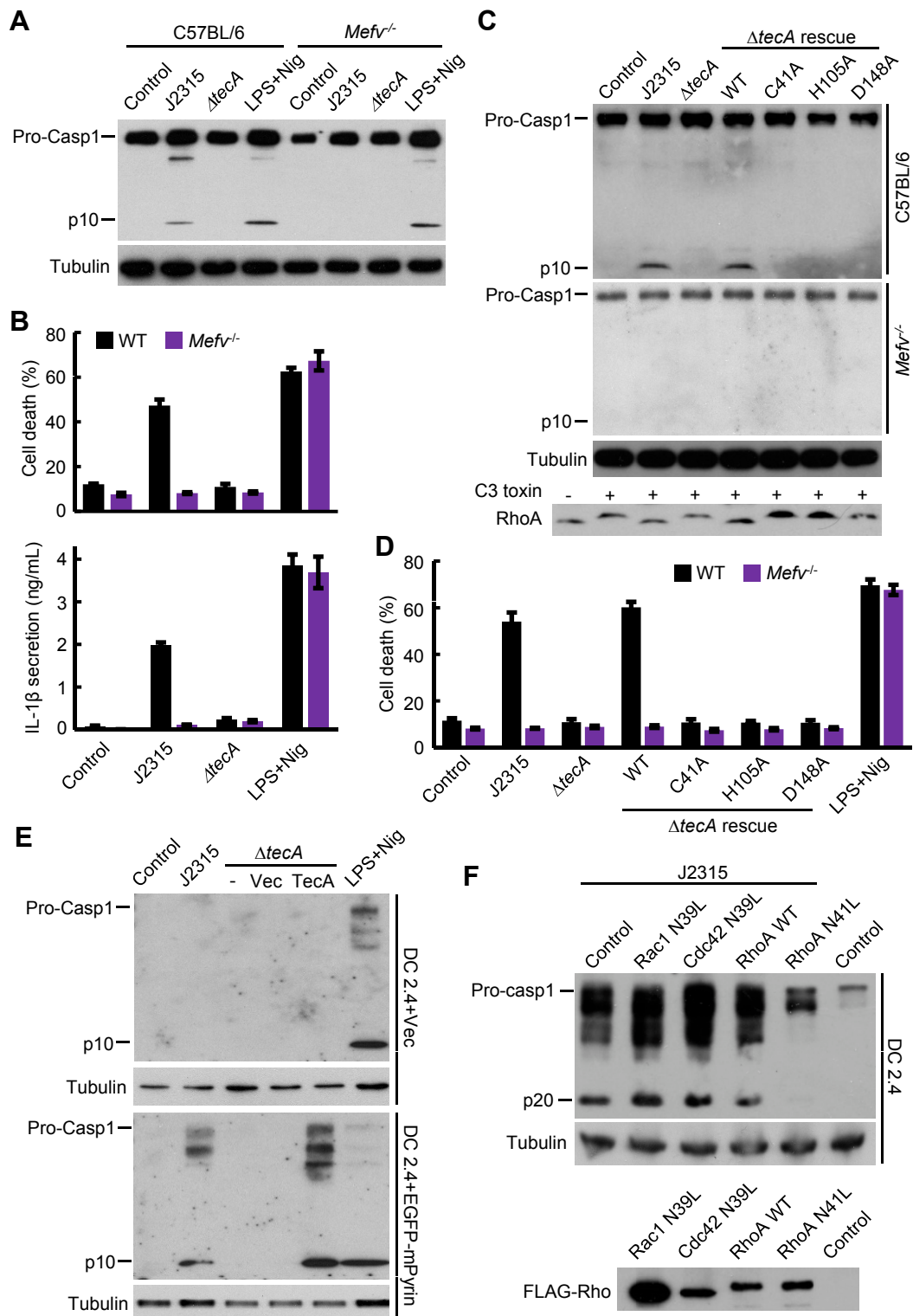


Figure 7. The Rho Deamidase Activity of TecA Triggers Inflammation and Its Recognition by Pyrin Protects Mice from Lethal *B. cenocepacia* Infection

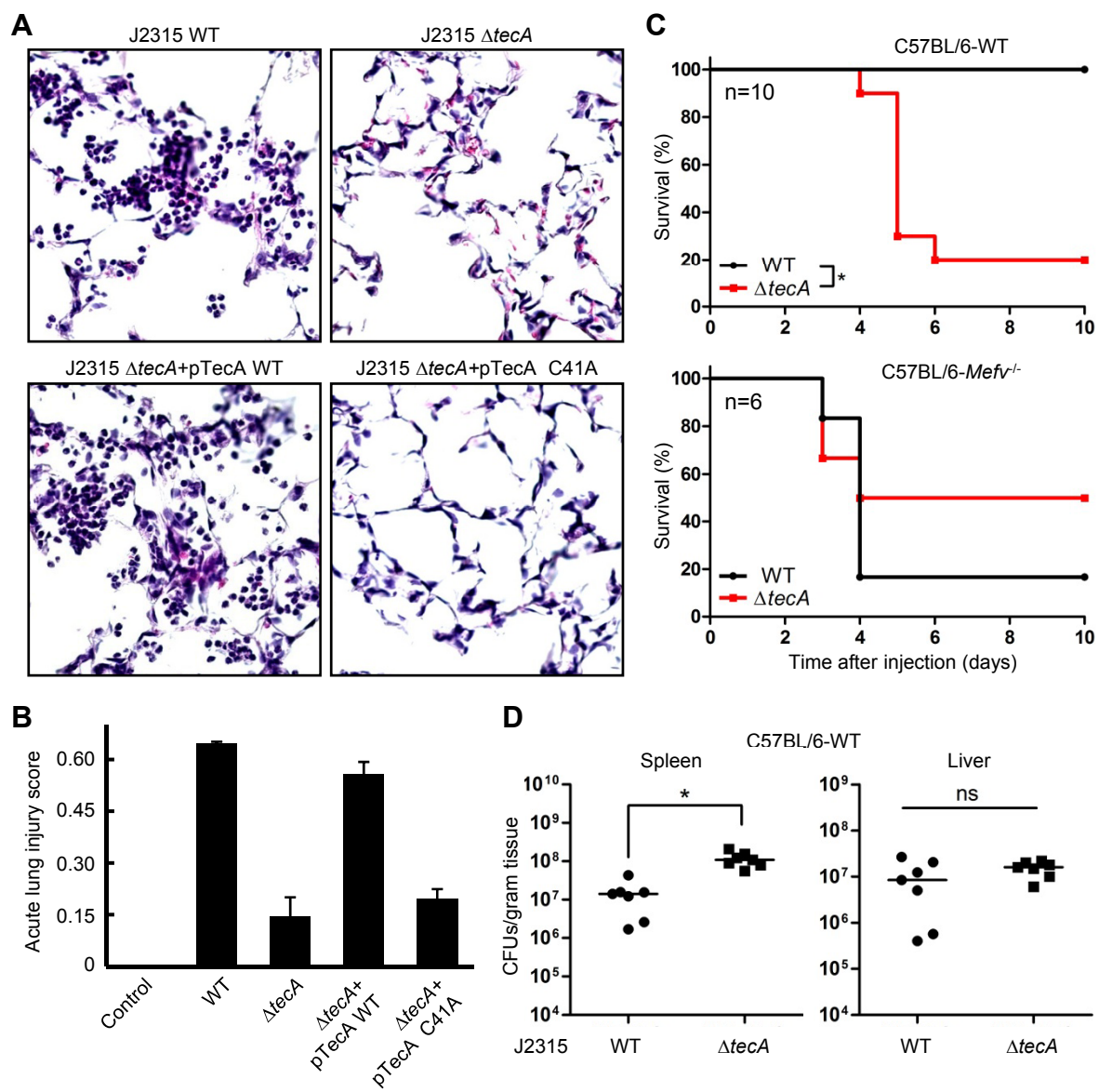


Figure S1. Characterization of *B. cenocepacia* K56-2 $\Delta tecA$ Mutant and T6SS-dependent TecA Secretion

